Electronic Supplementary Material (ESI) for RSC Advances.

Effect of pendant isophthalic acid moieties on the adsorption properties of light hydrocarbons in HKUST-1-like tbo-MOFs: Application to methane purification and storage

Youssef Belmabkhout,[a#] Hasnaa Mouttaki,[b#] Jarrod F. Eubank,[b,c] Vincent Guillerm,[a] and Mohamed Eddaoudi*[a,b]

[a]Functionnal Materials Design, Discovery and Development (FMD^3), Advanced Membrane and Porous Materials Center (AMPM), Division of Physical Science and Engineering, King Abdullah University of Science and Technology (KAUST), Thuwal 23955-6900, Kingdom of Saudi Arabia

[b]Department of Chemistry, University of South Florida, 4202 East Fowler Avenue (CHE 205), Tampa, FL 33620, USA

[c]Department of Chemistry and Physics, Florida Southern College, 111 Lake Hollingsworth Dr., Lakeland, FL, USA 33801

E-mail: mohamed.eddaoudi@kaust.edu.sa

# These authors contributed equally.

Electronic Supplementary Information

Table of Content

Electronic Supplementary Information

tbo-**MOF-2 and** tbo-**MOF-3**

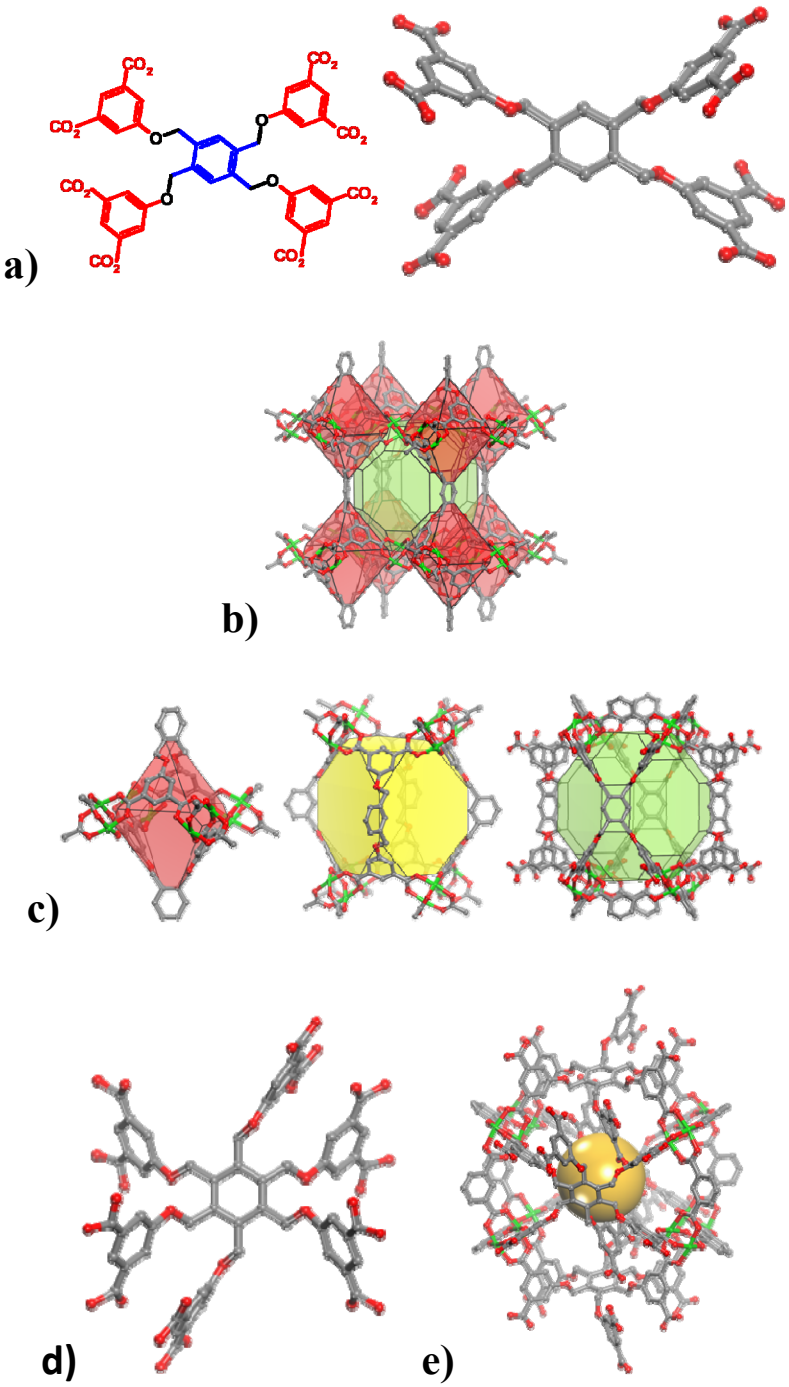

Fig.Fig. S1 a) L1: The ligand in **tbo**-MOF-2 is constructed from tetra-isophthalate termini (red) connected through alkoxy (i.e., methoxy) links (black) to a 4-connected benzene core (blue). b) Representative section from the crystal structure of 3-periodic **tbo**-MOF-2, showing polyhedral cages. c) Each type of polyhedral cage in **tbo**-MOF-2; truncated tetrahedron (red), truncated cube (yellow), and truncated cuboctahedron (green). d) L2: Functionalized version of L1, with pendant isophthalate moieties at the 3- and 6- positions. e) Representation of the largest cage from the 3-periodic **tbo**-MOF-3; the open space is reduced due to pendant groups, as indicated by the relatively small vdW sphere.

Electronic Supplementary Information

N_2 adsorption at 77 K

For sorption measurements, each compound, **tbo**-MOF-2 and **tbo**-MOF-3, were loaded into a sample cell wet, excess solvent was decanted using a syringe and then any remaining solvent was evaporated by allowing a continuous flow of N_2 to pass through the sample cell. Then, the sample was loaded onto the degasser.

Gas sorption measurements were conducted on the fully-evacuated **tbo**-MOFs after exchanging the guest molecules in **tbo**-MOF-2 and **tbo**-MOF-3 with CH_3CN and chloroform, respectively for 5 days. The argon sorption isotherms for both materials revealed reversible type I isotherms, which are characteristic of microporous materials (Fig. S2).

The pore size distribution, calculated from the Ar isotherms, revealed the presence of three distinct pore sizes, which correspond to the truncated tetrahedron, truncated cube, and truncated cuboctahedron. Accordingly, the estimated diameter of the cages is 7.7, 11.2 and 14.5 Å in **tbo**-MOF-2 and 7.2, 9.6 and 10.8 Å in **tbo**-MOF-3.

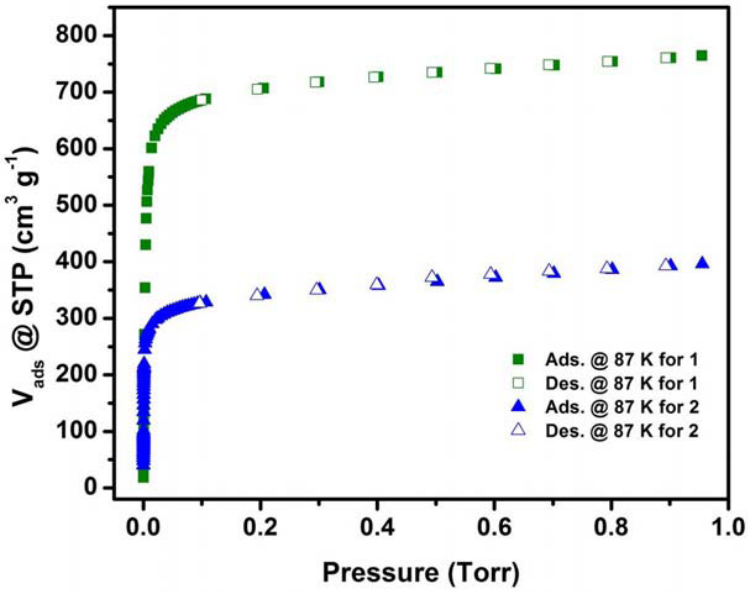

Fig. S2 Adsorption-desorption isotherms of Ar on the parent, **tbo**-MOF-2 (1), and **tbo**-MOF-3 (2).

Electronic Supplementary Information

Adsorption isotherms of CO_2, CH_4, C_2H_6, C_2H_4, C_3H_8, and C_3H_6

Adsorption equilibrium measurements of pure gases were performed using a Rubotherm gravimetric-densimetric apparatus (Bochum, Germany) (Scheme S1), composed mainly of a magnetic suspension balance (MSB) and a network of valves, mass flow meters, and temperature and pressure sensors. The MSB overcomes the disadvantages of other commercially available gravimetric instruments by separating the sensitive microbalance from the sample and the measuring atmosphere, and is able to perform adsorption measurements across a wide pressure range (i.e., from 0 to 20 MPa). The adsorption temperature may also be controlled within the range of 77 K to 423 K. In a typical adsorption experiment, the adsorbent is precisely weighed and placed in a basket suspended by a permanent magnet through an electromagnet. The cell in which the basket is housed is then closed and vacuum or high pressure is applied. The gravimetric method allows the direct measurement of the reduced gas adsorbed amount (Ω). Correction for the buoyancy effect is required to determine the excess and absolute adsorbed amount using equations 1 and 2, where $V_{adsorbent}$ and V_{ss} and $V_{adorbed\ phase}$ refer to the volume of the adsorbent, the volume of the suspension system, and the volume of the adsorbed phase, respectively.

$$\Omega = m_{absolute} - \rho_{gas}(V_{adsorbent} + V_{ss} + V_{adsorbed-phase}) \quad (1)$$

$$\Omega = m_{excess} - \rho_{gas}(V_{adsorbent} + V_{ss}) \quad (2)$$

The buoyancy effect resulting from the adsorbed phase may be taken into account via correlation with the pore volume or with the theoretical density of the sample.

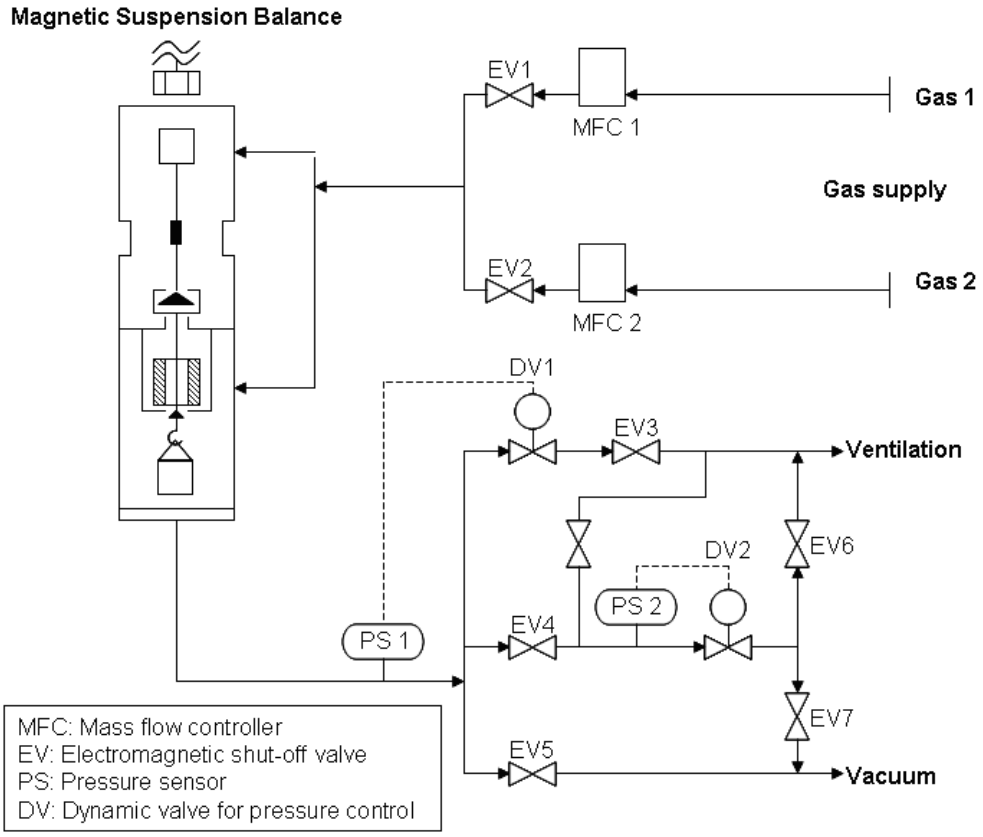

Scheme S1 Representation of the Rubotherm gravimetric-densimetric apparatus.

These volumes are determined using the helium isotherm method by assuming that helium penetrates in all open pores of the materials without being adsorbed. The density of the gas is determined using the Refprop equation of state (EOS) database and checked experimentally using a volume-calibrated titanium cylinder. By weighing this calibrated volume in the gas atmosphere, the local density of the gas is also determined. Simultaneous measurement of adsorption capacity and gas-phase density as a function of pressure and temperature is therefore possible.

The pressure is measured using two Drucks high pressure transmitters ranging from 0.5 to 34 bar and 1 to 200 bar, respectively, and one low pressure transmitter ranging from 0 to 1 bar. Prior to each adsorption experiment, about 200 mg of sample is outgassed at 473 K at a residual pressure of 10^{-6} mbar. The temperature during adsorption measurements is held constant by using a thermostat-controlled circulating fluid.

Toth Model for single gas adsorption fitting

In the current work, the Toth model was used to fit the pure gas isotherms because of its suitable behavior at both low and high pressure and its simple formulation as expressed by equation 3 (Toth, 2002)[1]

$$n = n_s \frac{KP}{(1+(KP)^m)^{1/m}} \qquad (3)$$

where n is the amount adsorbed, n_s is the amount adsorbed at saturation, P is the equilibrium pressure, K is the equilibrium constant, and m is a parameter indicating the heterogeneity of the adsorbent.

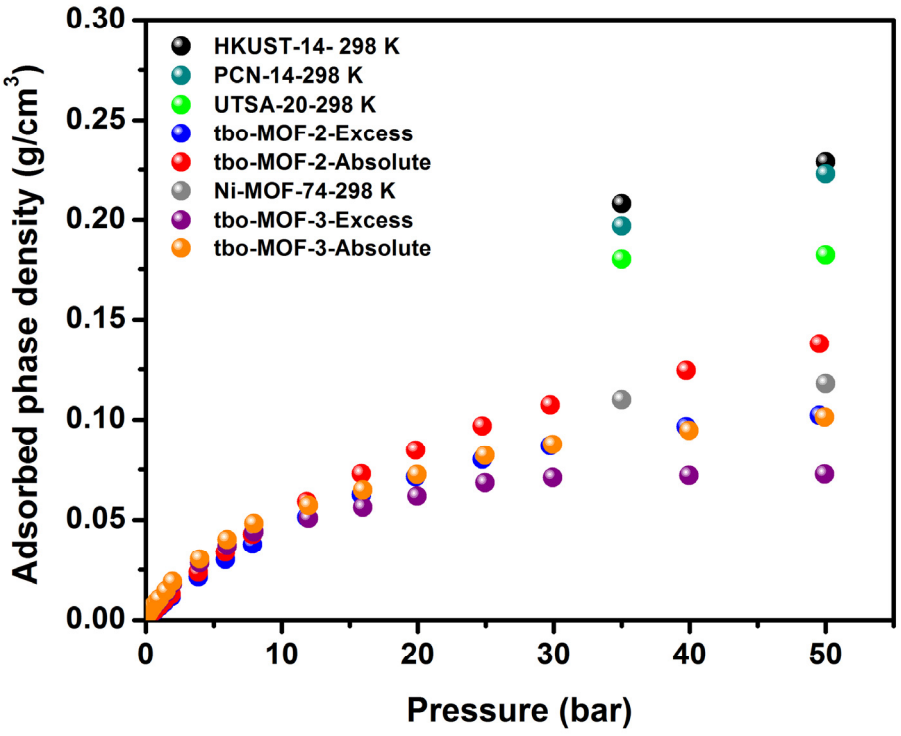

Fig. S3 Density of CH_4 (adsorbed phase) as a function of pressure in our **tbo**-MOFs compared to the corresponding data for the best (methane storage) MOFs reported so far (UTSA-20,[2] PCN-14,[3] Ni-MOF-74,[4] and **tbo**-MOF-1 (HKUST-1)[4]).

Table S1 Volumetric CH_4 working capacity using adsorption and desorption at 5 bar and 35 bar, respectively, for **tbo**-MOF-2, **tbo**-MOF-3, UTSA-20,[2] PCN-14,[3] Ni-MOF-74,[4] **gea**-MOF-1[5] and **tbo**-MOF-1 (HKUST-1)[4].

Adsorbent	Estimated CH_4 adsorption uptake at 5 bar cm^3 (STP)/cm^3	Estimated CH_4 adsorption uptake at 35 bar cm^3 (STP)/cm^3	Working storage uptake cm^3 (STP)/cm^3
tbo-MOF-2	40	160	120
tbo-MOF-3	50	125	75
UTSA-20	100	180	80
PCN-14	75	190	115
Ni-MOF-74	105	225	120
gea-MOF-1	40	140	100
HKUST-1 (**tbo**-MOF-1)	75	225	150

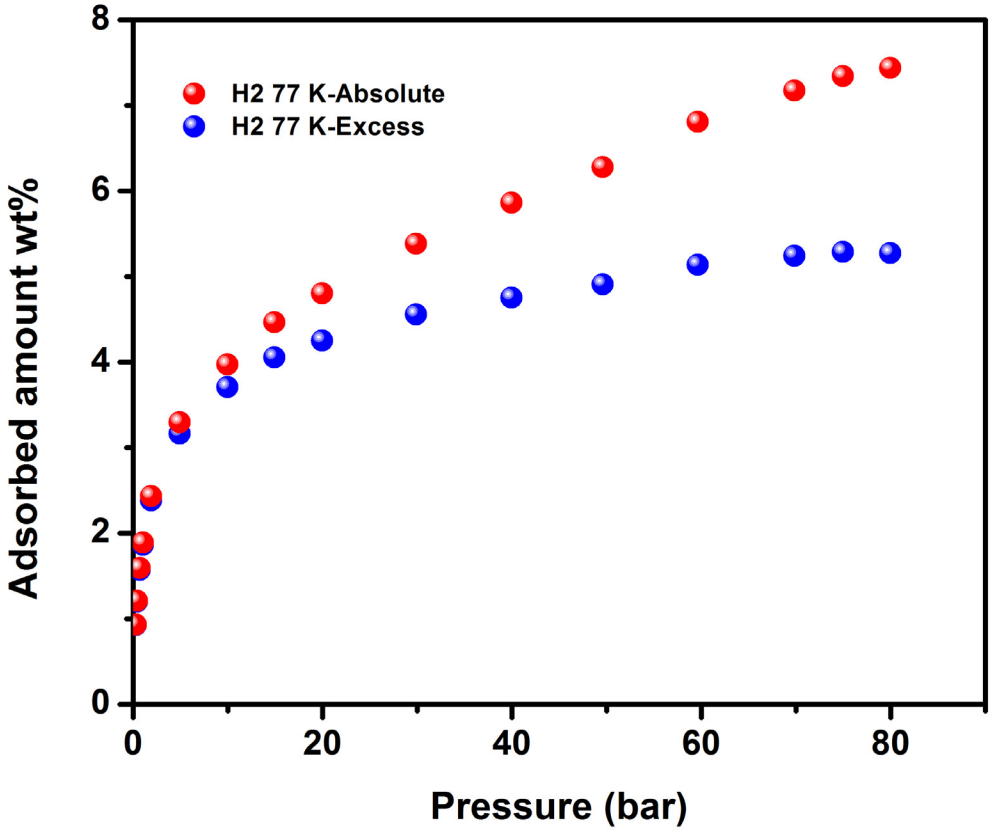

Fig. S4 High pressure hydrogen adsorption at 77 K of the parent **tbo**-MOF-2.

Electronic Supplementary Information

Physical-chemical properties of probe molecules and adsorption equilibrium data

Table S2 Physical-chemical properties of sorbates molecules (Li et al. 2009).[6]

Adsorbate	Kinetic diameter/ Å	Polarizability × 10^{25}/cm^3	Dipole moment × 10^{18}/ esu cm	Quadrupole moment × 10^{26}/ esu cm^2
CH_4	3.76	25.93	0	0
CO_2	3.3	29.11	0	4.3
C_2H_6	4.44	44.3-44.7	0	0.65
C_2H_4	4.16	42.52	0	1.5
C_3H_8	5.12	62.9-93.7	0.084	0
C_3H_6	4.67	62.6	0.366	0

Table S3 Toth parameters for adsorption on **tbo**-MOFs.

	Parameters	Gases						
		CH_4	**C_2H_6**	**C_2H_4**	**C_3H_6**	**C_3H_8**	**CO_2**	**N_2**
tbo-MOF-2	n_s	28.4420	12.0384	20	12.3153	10.4040	20.3923	12.733
	K	**0.0869**	**0.51441**	**1.0258**	**12.8020**	**6.9220**	**0.1410**	**0.0184**
	m	0.5113	1.6757	0.5358	0.71738	1.2296	1.2973	0.7395
tbo-MOF-3	n_s	5.4277	5.4256	6.3450	5.9300	5.2637	9.1795	11.6940
	K	**0.1275**	**2.3898**	**2.0544**	**56.8600**	**65.2091**	**0.5205**	**0.03541**
	m	0.9822	0.7827	0.6599	0.4500	0.9161	0.8091	0.4234

Prediction of multicomponent gas adsorption Ideal Adsorption Solution Theory (IAST)

The Ideal Adsorption Solution Theory (IAST) proposed by Mayer and Prausnitz (1965)[7] uses pure gas adsorption isotherms to predict the mixture adsorption equilibrium at the temperature of interest. For IAST application, the main condition to be fulfilled is the availability of (i) good quality single component adsorption data of different gases, and (ii) an excellent curve fitting model for such data (Chen and Sholl, 2007; [8] Bae et al., 2008[9]). In the current work, MSL and DSL models were used to fit the pure gas isotherms, as mentioned earlier

The most important equations used in the IAST calculation are listed hereafter:

$$f_i = x_i f_i^0(\pi) \tag{3}$$

$$\frac{\pi A}{RT} = \int_0^{f_i^0} n_i d\ln f_i \tag{4}$$

$$\frac{1}{n_t} = \sum_i \frac{x_i}{n_i^0} \tag{5}$$

$$S_{CO_2-i} = \frac{x_{CO_2}/x_i}{y_{CO_2}/y_i} \tag{6}$$

where f_i is the fugacity of component i in the gas phase; f_i^0 is the standard-state fugacity (i.e., the fugacity of pure component *i* at the equilibrium spreading pressure of the mixture, π); x_i and y_i are the mole fractions of component i in the adsorbed and gas phase, respectively; A is the surface area of the adsorbent; n_i is the number of moles adsorbed of pure component *i* (i.e.,

the pure-component isotherm); and n_i^0 is the number of moles adsorbed of pure component *i* at the standard-state pressure.

Equation 3 is the central equation of IAST, specifying the equality of the chemical potential of component *i* in the gas and the adsorbed phase (which is assumed to be ideal in the sense of Raoult's law). Equation 4 allows the calculation of the spreading pressure from the pure-component adsorption isotherm. The total amount adsorbed of the mixture, n_t, and the selectivity of CO_2 with respect to *i*, S_{CO_2-i}, are given by equations 5 and 6, respectively. The selectivity, S_{CO_2-i}, reflects the efficiency of CO_2 separation.

Binary gas mixture adsorption prediction using Ideal Adsorption Solution Theory (IAST)

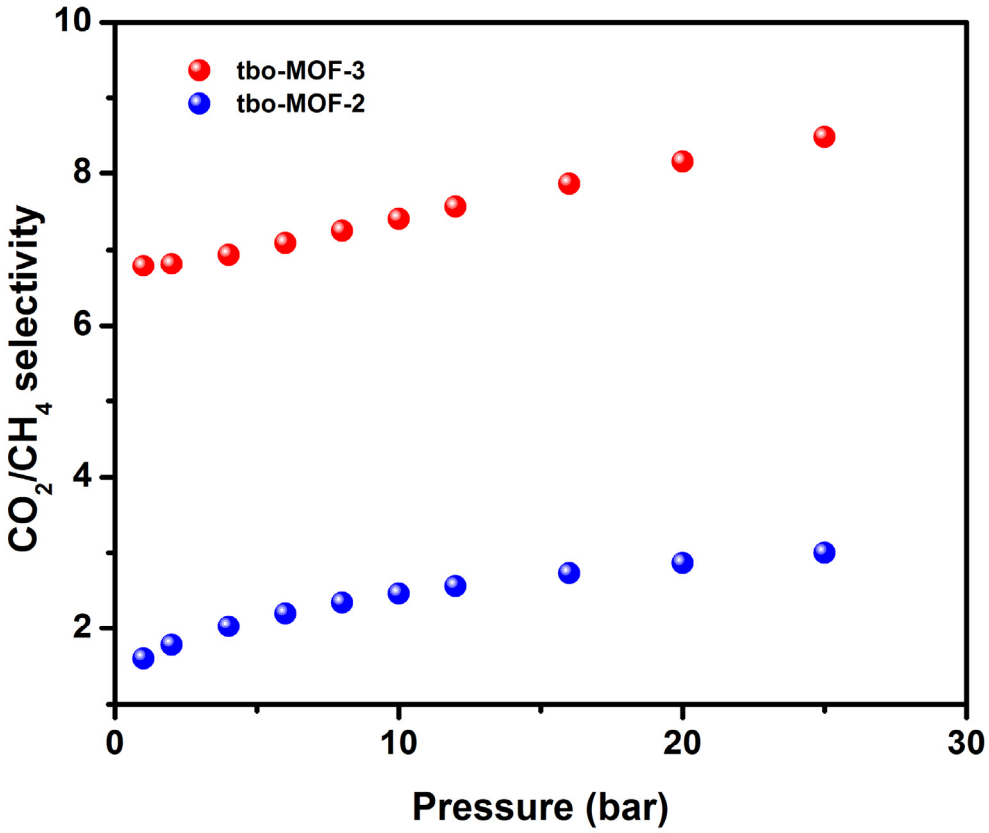

Fig. S5 CO_2 selectivity over CH_4 for CO_2/CH_4: 05/95 mixture on **tbo**-MOF-2 and **tbo**-MOF-3.

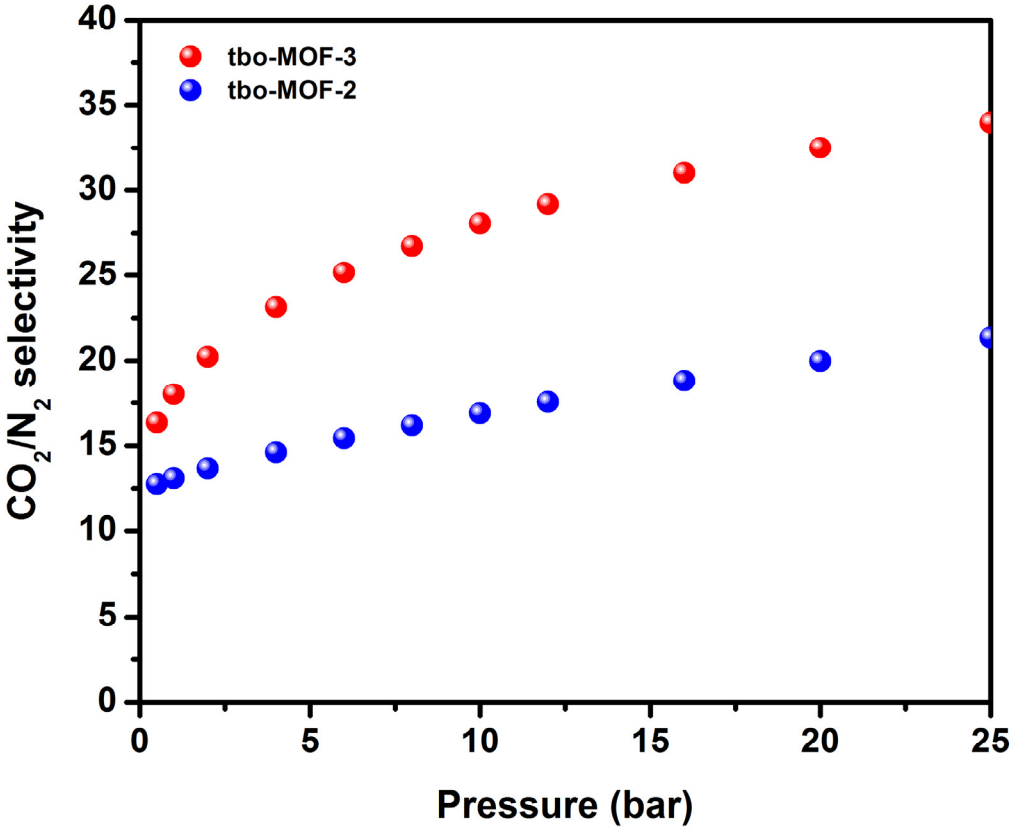

Fig. S6 CO_2 selectivity over N_2 for CO_2/N_2: 10/90 mixture on **tbo**-MOF-2 and **tbo**-MOF-3.

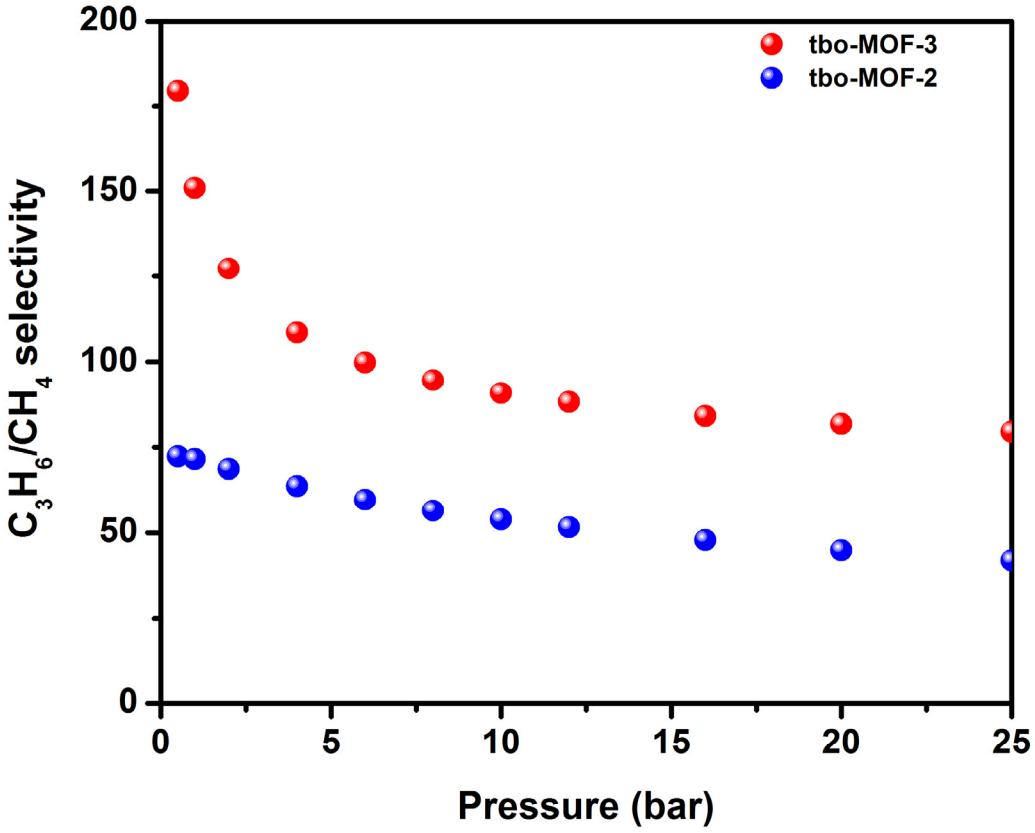

Fig. S7 C_3H_6 selectivity over CH_4 for C_3H_6/CH_4: 05/95 mixture on **tbo**-MOF-2 and **tbo**-MOF-3.

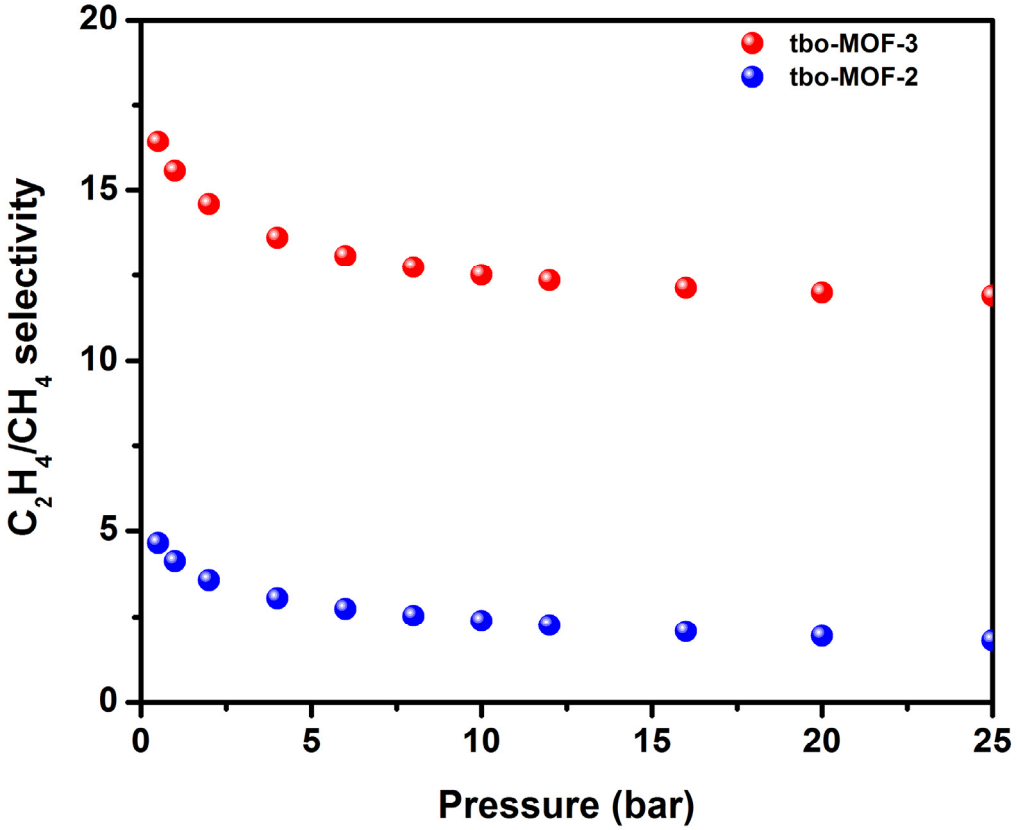

Fig. S8 C_2H_4 selectivity over CH_4 for C_2H_4/CH_4: 05/95 mixture on **tbo**-MOF-2 and **tbo**-MOF-3.

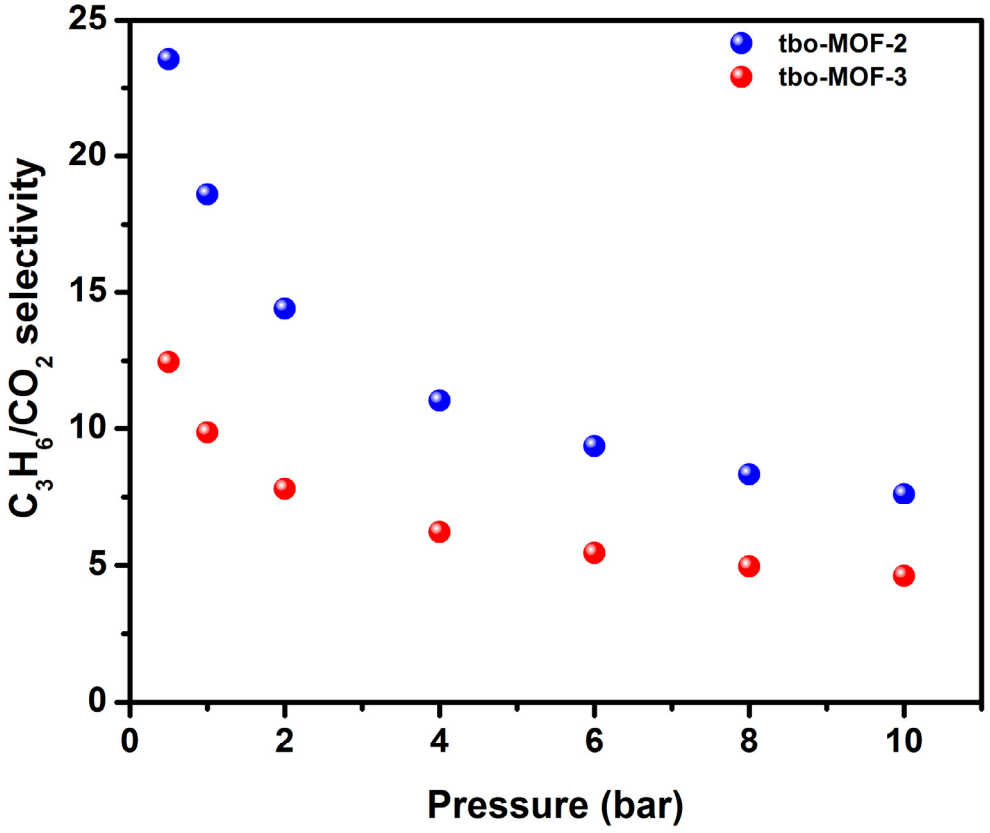

Fig. S9 C_3H_6 selectivity over CO_2 for C_3H_6/CO_2: 50/50 mixture on **tbo**-MOF-2 and **tbo**-MOF-3.

References

(1) Toth, J., 2002. Adsorption. Theory, modeling and analysis, Marcel Dekker, New York.

(2) Guo, Z.; Wu, H.; Srinivas, G. ; Zhou, Y.; Xiang, S.; Chen, Z.; Yang, Y.; Zhou, M.; O'Keeffe, M.; Chen, B. A metal-organic framework with optimized open metal sites and pore spaces for high methane storage at room temperature. *Angew. Chem. Int. Ed.* **2011**, *50*,3178-3181.

(3) Ma, S.; Sun, D.; Simmons, J. M.; Collier, C. D.; Yuan, D.; Zhou, H.-C. Metal-organic framework from an anthracene derivative containing nanoscopic cages exhibiting high methane uptake. *J. Am. Chem. Soc.* **2008**, *130*, 1012-1016

(4) Peng, Y.; Krungleviciute, V.; Eryazici, I.; Hupp, J.T.; Farha, O. K.; Yildirim, T. Methane storage in metal–organic frameworks: current records, surprise findings, and challenges. *J. Am. Chem. Soc.* **2013**, 135, 11887-11894.

(5) Guillerm, V.; Weseliński, Ł. J.; Belmabkhout, Y.; Cairns, A. J.; D'Elia, V.; Wojtas, Ł.; Adil, K.; Eddaoudi, M., Discovery and introduction of a (3,18)-connected net as an ideal blueprint for the design of metal‑organic frameworks. *Nat. Chem.* **2014**, *DOI:*10.1038/nchem.1982.

(6) Li, J.R.; Kuppler, R. J.; Zhou, H.C. Selective gas adsorption and separation in metal–organic frameworks. *Chem. Soc. Rev.* **2009**, 38, 1477–1504.

(7) Myers, A.L.; Prausnitz, J.M. Thermodynamics of mixed gas adsorption, *AIChE J.* **1965**,11, 121-127.

(8) Chen, H.; Sholl, D.S., Examining the accuracy of ideal adsorbed solution theory without curve fitting using transition Matrix Monte Carlo simulations. *Langmuir* **2007**, 23, 6431-6437.

(9) Bae, Y-S.; Mulfort, K.L.; Frost, H.; Ryan, P.; Punatahnam, S.; Braodbelt, L. J.; Hupp, J. T.; Snurr, Q.R. Separation of CO_2 and CH_4 using mixed-ligand metal-organic frameworks. *Langmuir* **2008**, *24*, 8592-8598.